Microlocally correct photoacoustic reconstructions from spatially reduced data

Philip Hoskins

University of Arizona

February 28, 2020

Joint work with L. Kunyansky (Arizona) and M. Eller (Georgetown)

Supported in part by NSF/DMS-1814592

Medical imaging and tomography

Goal: Create images to "see" inside the body without surgery

- Images are a snapshot of some physiological structure or process
- Used to aid in diagnosis and therapy

To obtain an image, a signal (i.e. waves, particles) is passed through the object and is picked up by a scanner (measuring device)

Direct Imaging vs Tomography

- In direct imaging, measurements form the image (e.g. photography, X-ray radiography, ultrasound sonography)
- In tomography, image is reconstructed by solving an inverse problem with measurements as data

Four examples of imaging modalities

Cat scan with X-ray CT

MRI scanner

Ultrasound

Note the donut shape of the CT and MRI scanners!

The need for more modalities

- No modality can image all pathologies
- Tradeoffs between cost, speed, exposure to radiation

Ex: Some tissue pathologies (cancer) are more conductive than healthy tissue $\implies$ Try to image conductivity?

Medical electrical impedance tomography developed
unstable inverse problem $\implies$ blurry images $\implies$ not practical

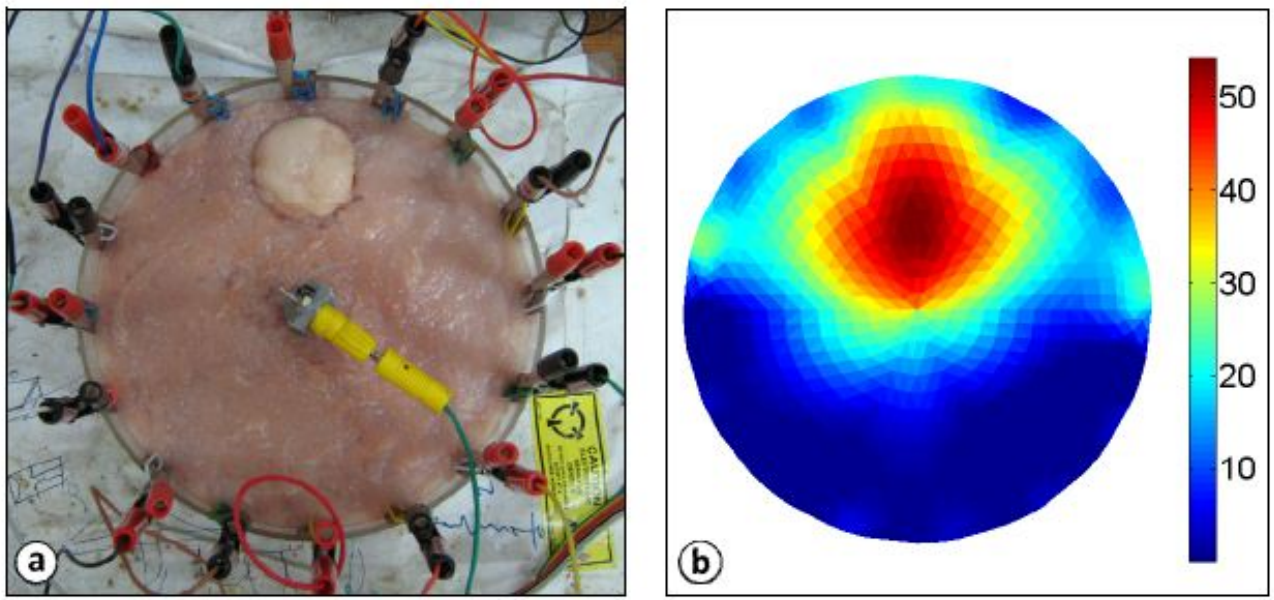

EIT image of chicken tissue

Emerging coupled-physics modalities

New idea: Combine a high resolution wave (e.g.,ultrasound) with a wave sensitive to the desired property we want to image, such as conductivity or optical absorption (EM waves)

Ultrasound-based coupled-physics imaging modalities:

- Photoacoustic tomography
- Thermoacoustic tomography
- Magnetoacoustoelectric tomography

There are many others, but the above all require solving an inverse source problem for the wave equation, which we will investigate in this talk

Photoacoustic/Thermoacoustic tomography

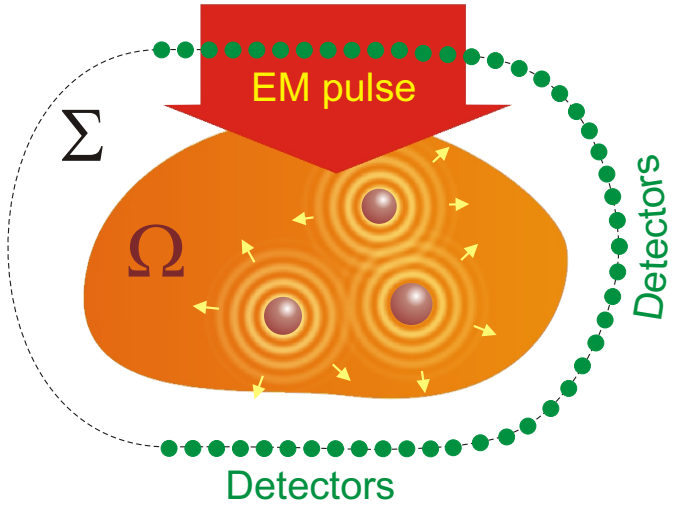

Schematic of PAT/TAT procedure

- Laser beam irradiates tissue (microwave in TAT), causing a small level of heating inside
- Thermoelastic expansion results in propagating pressure wave
- Acoustic transducers measure time-dependent pressure $u(t, x)$ on some surface Σ at least partially surrounding the object
- Initial pressure $u(0, x)$ contains useful diagnostic information (much higher in cancerous cells)

Mathematical model for PAT

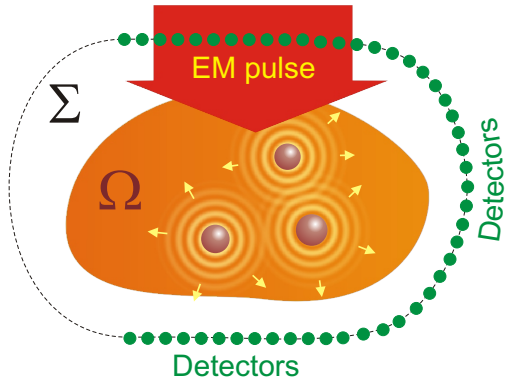

Usually, it's assumed that the initial pressure $f(x)$ is supported inside a bounded region Ω surrounded (at least partially) by a finite surface (curve in 2D) Γ. The pressure $u(t,x)$ is described by the wave equation with Cauchy data

$$\begin{cases} \Delta u(t,x) = \frac{1}{c(x)^2} u_{tt}(t,x), \quad t \geq 0, x \in \mathbb{R}^d \\ u(0,x) = f(x) \\ u_t(0,x) = 0 \end{cases}$$

Inverse problem: recover $f(x)$ from data

$$g(t,z) = u(t,z), \quad t \geq 0, z \in \Gamma$$

Reconstruction methods

1. Explicit inversion formulas
   - known for certain problems with full data [closed observation surface (curve in 2D)] and acoustically homogeneous media (speed of sound $c(x)$ is constant)
   - circles, ellipses, squares, cylinders, spheres, cubes, ellipsoids
   - Fast and accurate implementations, but narrow applicability
2. Iterative techniques
   - do not suffer from some of the defects of explicit inversion formulas
   - slow and computationally expensive, particularly for problems with partial data
3. Eigenfunction expansions
   - fast implementations for circles, spheres, and cylinders

Analytic methods for partial data (finite, open observation surface/curve) have received less attention. This is the problem we want to investigate.

Introduce Radon transform

- Maps a function $q(x)$ to its integral over a hyperplane $L = \{x \mid x \cdot \omega = p\}$

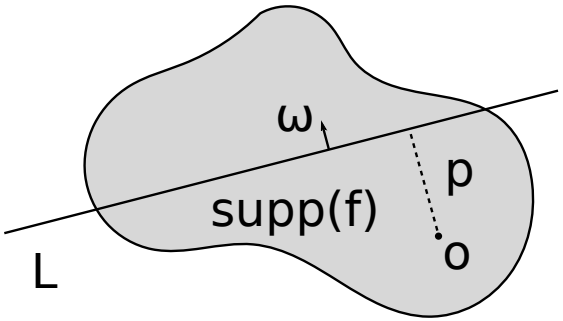

- Parameterization L: $x \cdot \omega = p$, $\omega \in \mathbb{S}^{d-1}$, $p \in \mathbb{R}$

$$h(\omega, p) := \mathcal{R}q(\omega, p) = \int_{\mathbb{R}^d} q(x)\delta(x \cdot \omega - p)dx$$

where $\delta(\cdot)$ is the Diract delta

The values $h(\omega, p)$ are called Radon projections of $q(x)$. $h(\omega, p)$ defines a function on the cylinder $\mathbb{S}^{d-1} \times \mathbb{R}$ with the symmetry $h(\omega, p) = h(-\omega, -p)$.

Inversion formula for Radon transform

This is the well-known filtered backprojection (FBP) formula. Methods for implementing this formula have been extensively studied

1. Define the Hilbert transform $\mathcal{H}$ of a 1D function $h(t)$ by

$$\mathcal{H}(s) = \text{p.v.} \int_{\mathbb{R}} \frac{h(t)}{s-t} dt$$

2. The adjoint $\mathcal{R}^{\#}$ of the the Radon transform (aka backprojection) is

$$\mathcal{R}^{\#} h(x) = \int_{\mathbb{S}^{d-1}} h(\omega, \omega \cdot x) d\omega$$

The inverse Radon transform $\mathcal{R}^{-1}$ is defined by

$$\mathcal{R}^{-1} F(x) = \frac{1}{2(2\pi)^{d-1}} \begin{cases} (-1)^{\frac{d-2}{2}} \left[\mathcal{R}^{\#} \mathcal{H} \frac{\partial^{d-1} F}{\partial p^{d-1}} \right](x), & d \text{ is even} \\ (-1)^{\frac{d-1}{2}} \left[\mathcal{R}^{\#} \mathcal{H} \frac{\partial^{d-1} F}{\partial p^{d-1}} \right](x), & d \text{ is odd} \end{cases}$$

If $F(\omega, p) = \mathcal{R} f(\omega, p)$, then $f(x) = \mathcal{R}^{-1} F(x)$.

Inverse source problem with partial data and homogeneous media

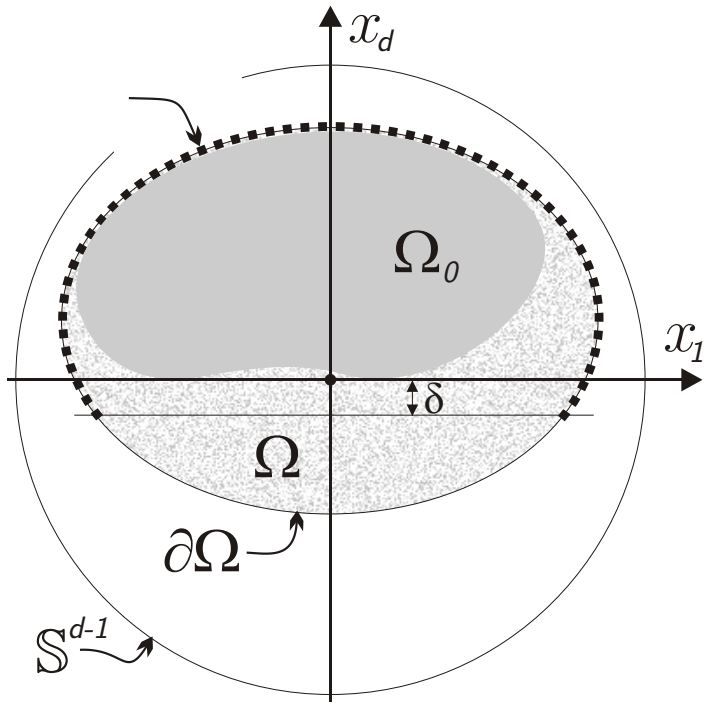

Assumptions:

- The support of $f(x)$, denoted Ω_0, lies within convex region Ω_0 with smooth boundary $\partial\Omega$, contained in the unit sphere $\mathbb{S}^{d-1}$
- $\Gamma = \{x \mid x \in \partial\Omega \text{ and } x_d \geq -\delta\}$
- $c(x) \equiv 1$

Explicit reconstruction procedure

First introduce explicit procedure that is theoretically exact for complete data $g(t,z)$ for $z \in \partial\Omega$.

Step 1 Compute solution $w(t,x)$ of the exterior Dirichlet problem for the wave equation

$$\begin{cases} w_{tt}(t,x) = \Delta w(t,x) & (t,x) \in (0,\infty) \times (\mathbb{R}^d \setminus \overline{\Omega}) \\ w(0,x) = 0, w_t(0,x) = 0, & x \in \mathbb{R}^d \setminus \Omega \\ w(t,z) = g(t,z) & (t,z) \in (0,\infty) \times \partial\Omega \end{cases}$$

These are just the exterior values of the solution $u(t,x)$ of the Cauchy problem introduced earlier, with initial pressure $f(x)$

$$\begin{cases} u_{tt}(t,x = \Delta u(t,x), & t \geq 0, x \in \mathbb{R}^d \\ u(0,x) = f(x) \\ u_t(0,x) = 0 \end{cases}$$

I.e., $w(t,x) = u(t,x)$ when $x \in \mathbb{R}^d \setminus \Omega$.

Explicit reconstruction procedure cont...

Step 2 For each $t \geq 0$, define the Radon projections $\mathcal{R}u(t, \omega, p)$ and $F(\omega, p) = \mathcal{R}f(\omega, p)$. It can be shown that these solve the 1D wave equation

$$\begin{cases} \frac{\partial^2}{\partial t^2}\mathcal{R}u(t, \omega, p) = \frac{\partial^2}{\partial p^2}\mathcal{R}u(t, \omega, p) \\ \mathcal{R}u(0, \omega, p) = F(\omega, p), \frac{\partial}{\partial t}\mathcal{R}u(0, \omega, p) = 0 \end{cases}$$

This has solution

$$\mathcal{R}u(t, \omega, p) = \frac{1}{2}\left[F(\omega, p + t) + F(\omega, p - t)\right]$$

$F(\omega, p)$ vanishes outside $[-1, 1]$ in p, so for $t = 2$

$$F(\omega, p) = 2\mathcal{R}u(2, \omega, p + 2), \quad p \in [-1, 1]$$

Step 3 Recover $f(x)$ from $F(\omega, p)$ from FBP
More straightforward reconstructions are well-studied, but we want to apply this technique to reduced data!

Reconstruction from partial data

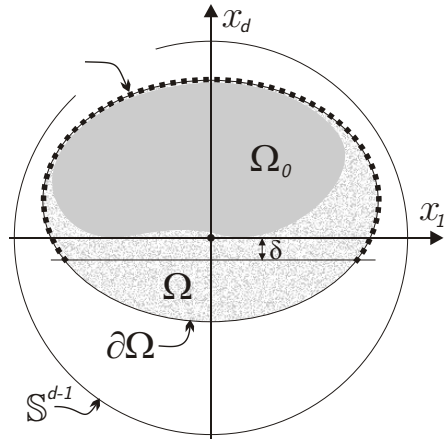

Consider the same problem, but the data $g(t, x)$ only given for $x \in \Omega$. Apply previously described procedure after first

1. Extending $g(t, x)$ to all of $\partial\Omega$ by 0
2. Multiplying $g(t, x)$ by a smooth cutoff function $\psi(x_3)$ such that

$$\begin{cases} \psi(x_3) = 1 & x_3 \geq 0 \\ \psi(x_3) = 0 & x_3 \leq -\delta \end{cases}$$

The procedure has to be applied with some slight modifications.

Continued...

In the partial data case, the exterior solution $w(t,x)$ serves as a crude approximation of the exact solution $u(t,x)$.

The exterior Radon projections

$$\tilde{F}(\omega,p) \equiv 2\mathcal{R}w(2,\omega,p+2), \quad p \in [-1,1]$$

are a poor approximation to $F(\omega,p)$. However, on the upper half sphere $\mathbb{S}_+^{d-1}$, $\tilde{F}(\omega,p) - F(\omega,p)$ is an infinitely smooth function. Instead apply FBP to

$$\check{F}(\omega,p) = \begin{cases} \tilde{F}(\omega,p), & \omega_d \geq 0 \\ \tilde{F}(-\omega,-p), & \omega_d < 0 \end{cases}$$

This yields an approximation to $f(x)$

$$\tilde{f}(x) = \mathcal{R}^{-1}\check{F}(x)$$

It will be shown in a future publication that

$$\tilde{f} - f \in C^\infty(B(0,1))$$

I.e., $\tilde{f}$ corresponds microlocally to $f(x)$.

What does microlocally accurate mean?

The gist: Location and size of sharp interfaces are reproduced correctly. Will see in numerical results why this is useful.

A function $f(x)$ is smooth near a point x_0 if and only if there is a $\phi(x) \in C_0^\infty(\mathbb{R}^d)$ with $\phi(x_0) \neq 0$ and for all positive integers N, the Fourier transform of ϕf satisfies

$$\hat{\phi f}(\xi) = O((1 + |\xi|)^{-N})$$

If the above holds in some conical neighborhood of a point $\xi_0 \in \mathbb{R}^d \setminus \{0\}$, then f is called microlocally smooth near (x_0, ξ_0).

The wavefront set $W(f)$ of a function characterizes the points in space and directions where a function fails to be smooth in the microlocal sense

The procedure described in the previous slides preserves the wavefront set of the initial pressure $f(x)$

Fast algorithm for the unit circle

Measuring surface is a part of the unit circle. Steps of the algorithm:

1. Compute solution $w(2, x)$ of the Dirichlet problem in the exterior of the unit disk $\mathbb{R}^2 \setminus B(0, 1)$
2. Compute Radon projections $\mathcal{R}w(2, \omega, p)$ on $\mathbb{S}^1_+ \times [1, 3]$

Separation of variables for the wave equation in polar coordiantes leads to

$$w(t, x) = w(t, r, \theta) = \int_{\mathbb{R}} \left[\sum_{k=-\infty}^{\infty} a_k(\lambda) H^{(1)}_{|k|}(r\lambda) e^{ik\theta} \right] e^{-i\lambda t} d\lambda$$

The Dirichlet condition is

$$w(t, 1, \theta) = g(t, \theta)$$

Only interested in $w(2, x)$, so can smoothly cut off $g(t, \theta)$ so that it is zero for all $t > 2 + b$

Fast algorithm cont...

Assuming $g(t,\theta)$ is sufficiently smooth, then

$$g(t,\theta) = \int_{\mathbb{R}} \left[\sum_{k=-\infty}^{\infty} b_k(\lambda) e^{ik\theta} \right] e^{-i\lambda t} d\lambda$$

where

$$b_k(\lambda) = \frac{1}{(2\pi)^2} \int_{-\pi}^{\pi} \left[\int_{\mathbb{R}} g(t,\theta) e^{i\lambda t} dt \right] e^{-ik\theta} d\theta$$

Since $w(t,1,\theta) = g(t,\theta)$, then

$$a_k(\lambda) = \frac{b_k(\lambda)}{H_{|k|}^{(1)}(\lambda)}, k \in \mathbb{Z}$$

Discretization of problem

Assume M point-like transducers placed along unit circle points $\theta_j = j\Delta\theta, j = -M/2, \ldots, M/2$

Measurements made at equispaced points in time $t_i = i\Delta t$, $i = 0, 1, \ldots, N$.

Approximate $b_k(\lambda)$ on grid of frequencies $\lambda_m = m\Delta\lambda, m = -m_{Nyq}, \ldots, m_{Nyq}$, where $m_{Nyq}\Delta\lambda$ is the Nyquist frequency of the time discretization

This can be done using FFTs with some zero-padding in the time dimension.

$$w(2, r, \theta) \approx \sum_{k=-M/2}^{M/2-1} \left[\sum_{m=-m_{Nyq}}^{m_{Nyq}-1} a_k(\lambda_m) H_{|k|}^{(1)}(r\lambda_m) e^{-2i\lambda_m} \right] e^{ik\theta}$$

Computing this series and then numerically evaluating its Radon transform is actually rather slow ... we can do better!

A truly fast algorithm

The Radon transform of circular wave functions $\psi_k^\lambda(r,\theta) = H_{|k|}^{(1)}(r\lambda)e^{ik\theta}$ can be computed explicitly. For $\omega(\alpha) = (\cos\alpha, \sin\alpha)$, $\alpha \in [-\pi, \pi]$

$$\mathcal{R}\psi_k^\lambda(\omega(\alpha), p) = 2\frac{(-i)^{|k|}}{\lambda}e^{i\lambda p}e^{ik\alpha}$$

Combining with the previous result gives

$$\mathcal{R}w(2,\omega(\alpha),p) \approx 2\sum_{k=-M/2}^{M/2-1}\left[\sum_{m=-m_{Nyq}}^{m_{Nyq}-1} a_k(\lambda_m)\frac{(-i)^{|k|}}{\lambda_m}e^{i\lambda_m(p-2)}\right]e^{ik\alpha}$$

Numerical simulations

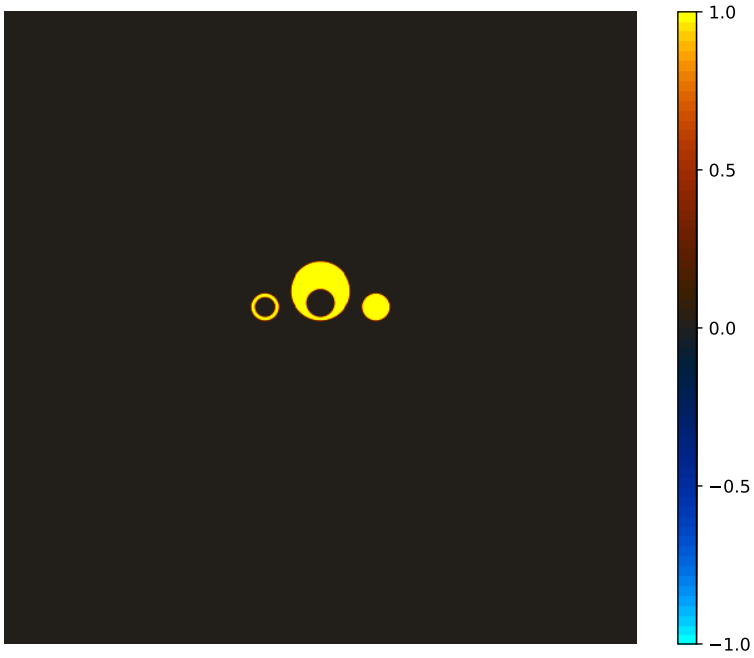

Initial condition $u(0, x)$ on $[-4, 4] \times [-4, 4]$

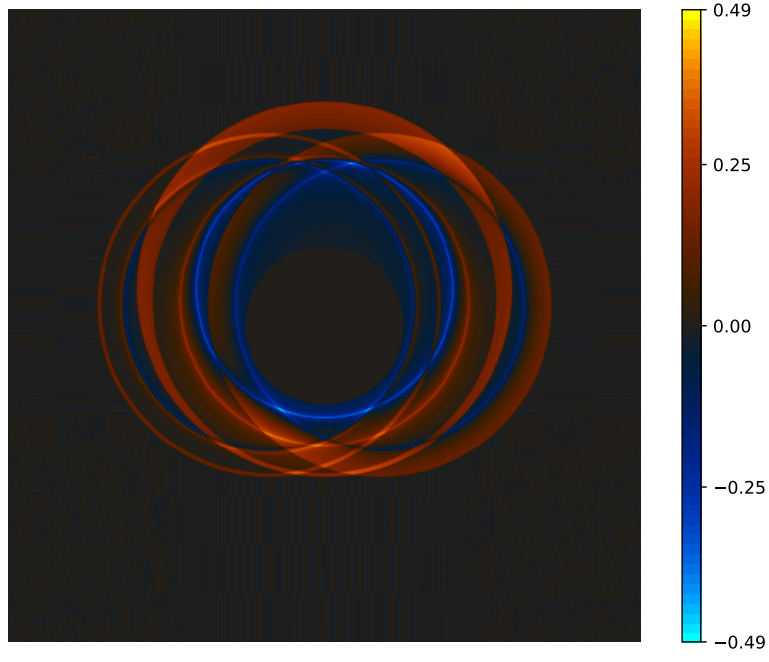

Direction solution at $t = 2$ with interior values cut out

Numerical simulations–data

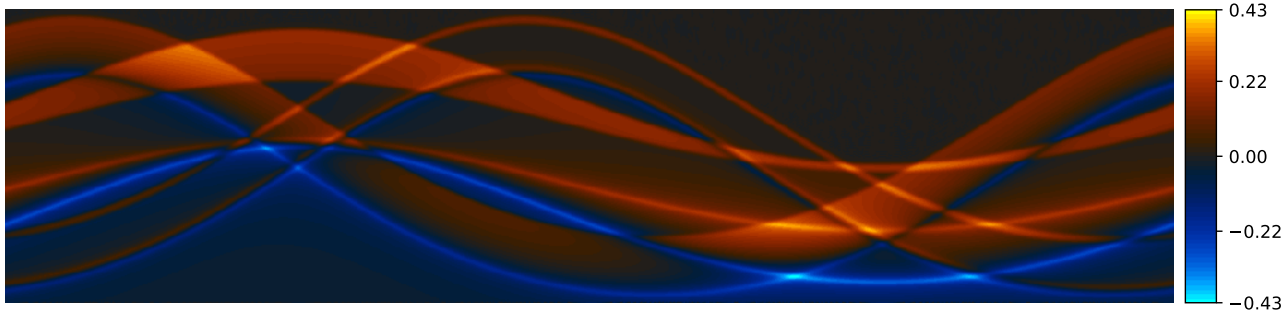

Direction solution at $t = 2$ in polar coordinates for $(\theta, r) \in [1, 3] \times [0, 2 * \pi]$

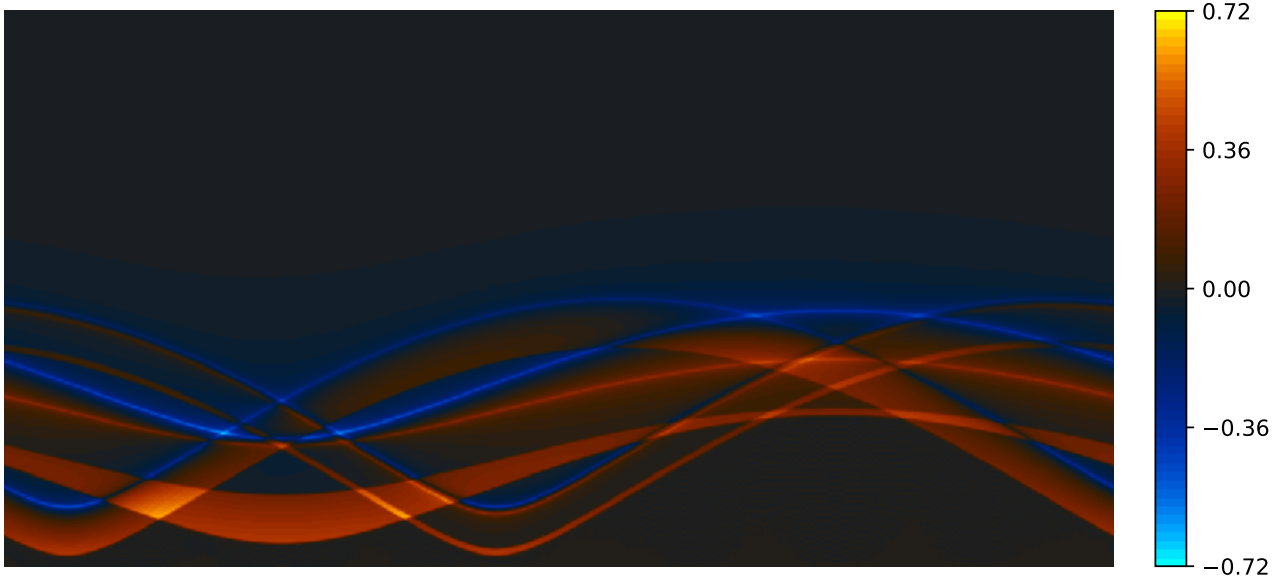

Boundary (unit circle) data for $(\theta, t) \in [0, 2\pi] \times [0, 4]$

Numerical simulations–reconstruction with full data

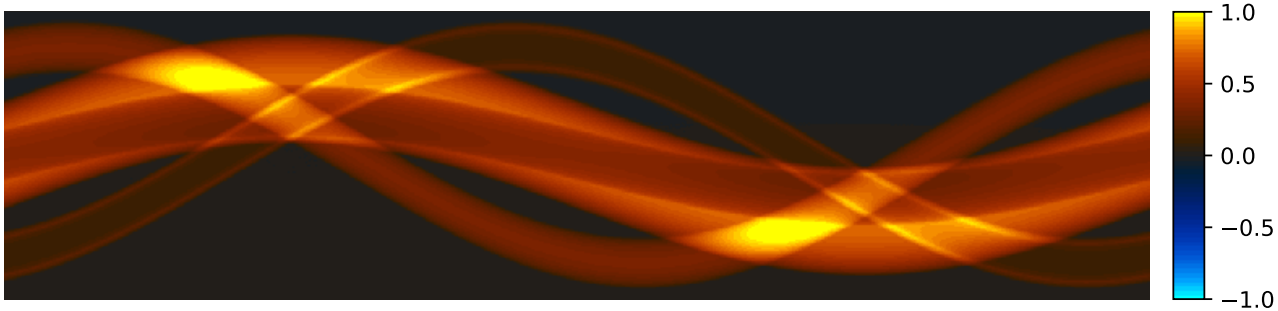

Reconstructed sinogram $F(\omega(\alpha), p)$ for $(\alpha, p) \in [0, 2\pi] \times [-1, 1]$

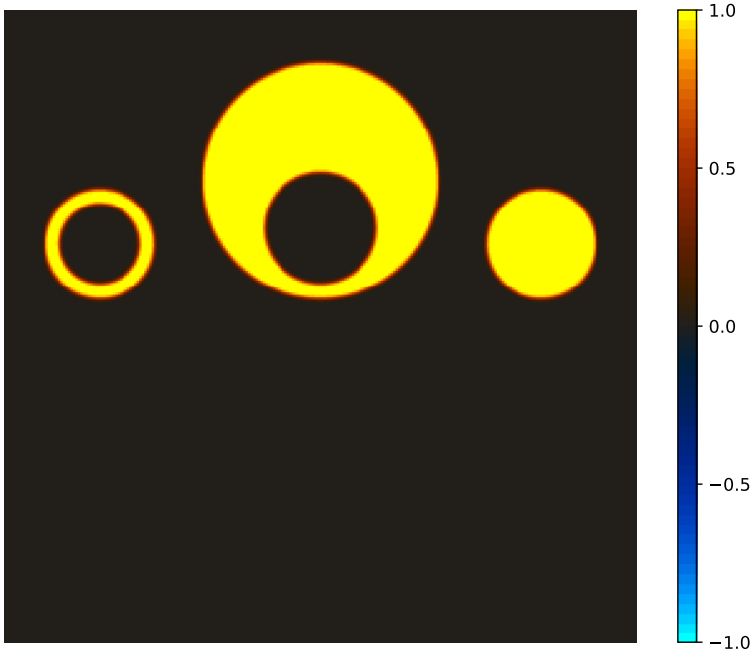

$f(x) = u(0, x)$ on unit square

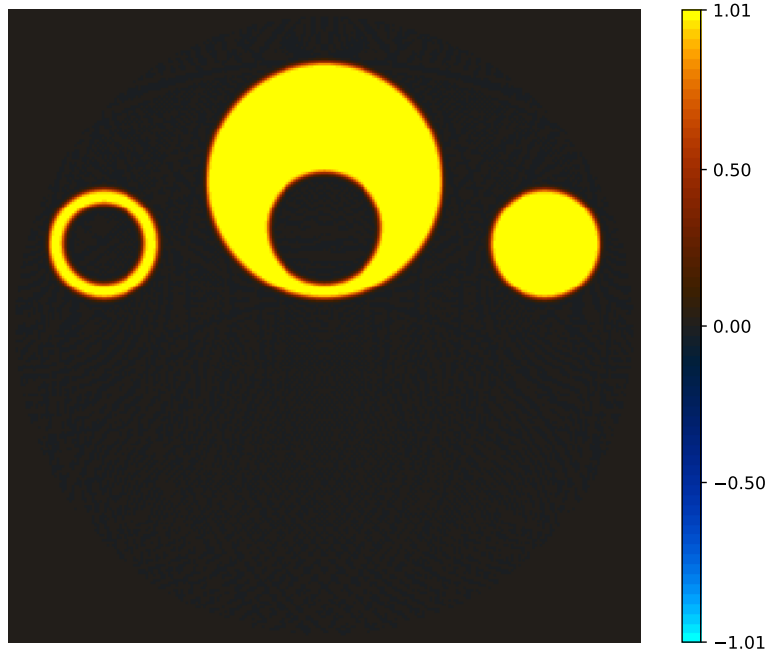

Reconstruction on unit square

cont...

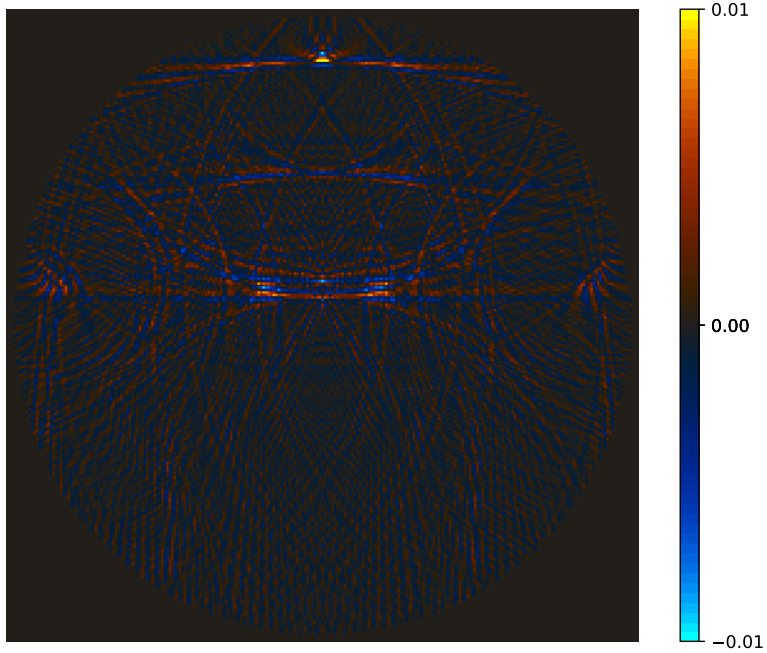

Difference between reconstructions from accurate sinogram and sinogram computed using our method

Numerical simulations–naive reconstruction

Reduced data $g(t, \theta)$ for $(\theta, t) \in [0, 2\pi] \times [0, 4]$

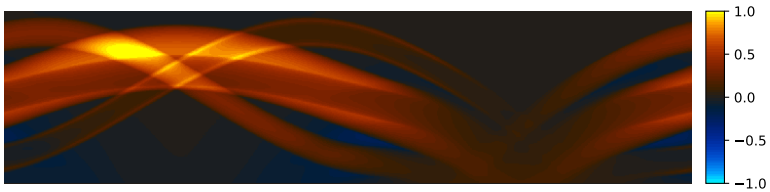

Sinogram computed from reduced data
$(\alpha, p) \in [0, 2\pi] \times [-1, 1]$

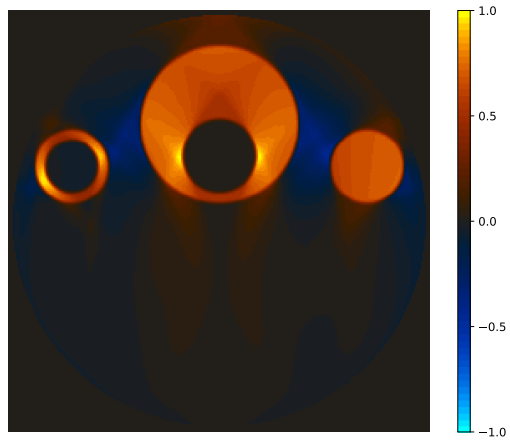

Naive reconstruction

Numerical simulations–reconstruction from partial data

Reduced data $g(t, \theta)$ for $(\theta, t) \in [0, 2\pi] \times [0, 4]$

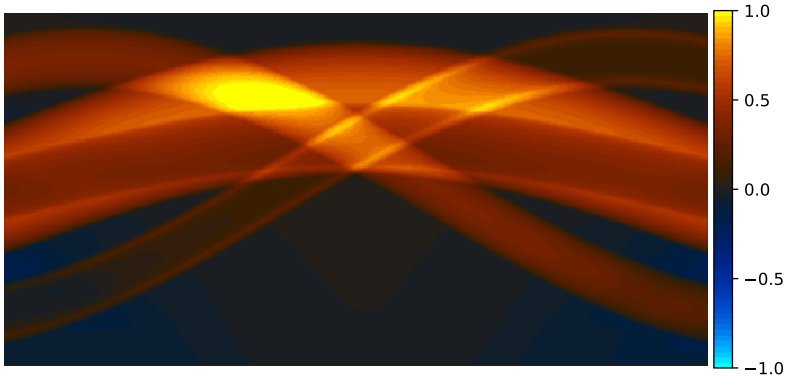

Sinogram computed from reduced data
$(\alpha, p) \in [0, \pi] \times [-1, 1]$

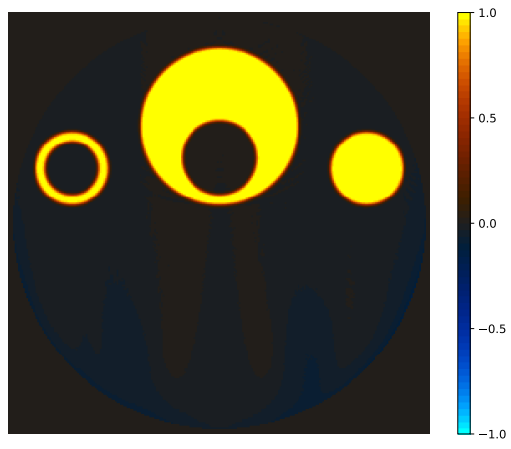

Smarter reconstruction

Numerical simulations–comparison with naive

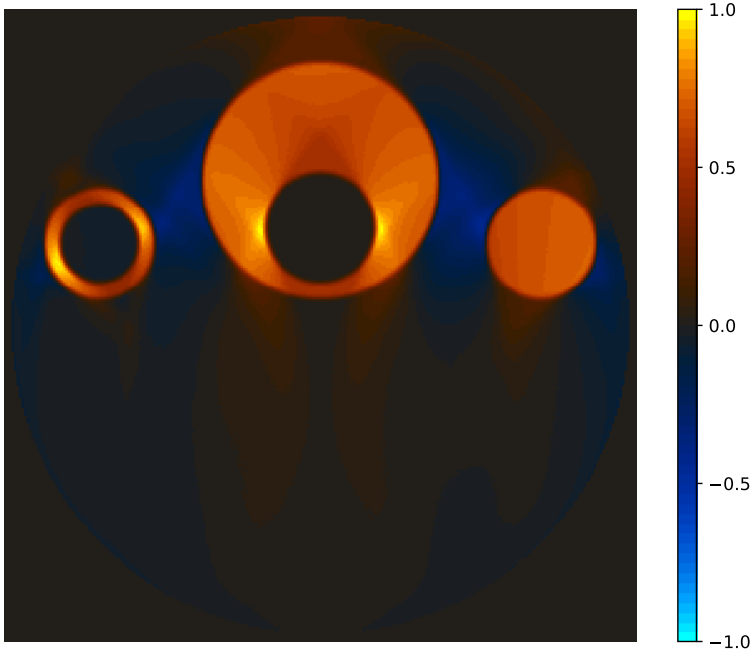

Naive reconstruction

Smarter reconstruction

This is the effect of preserving the wavefront set!

Numerical simulations–smooth error

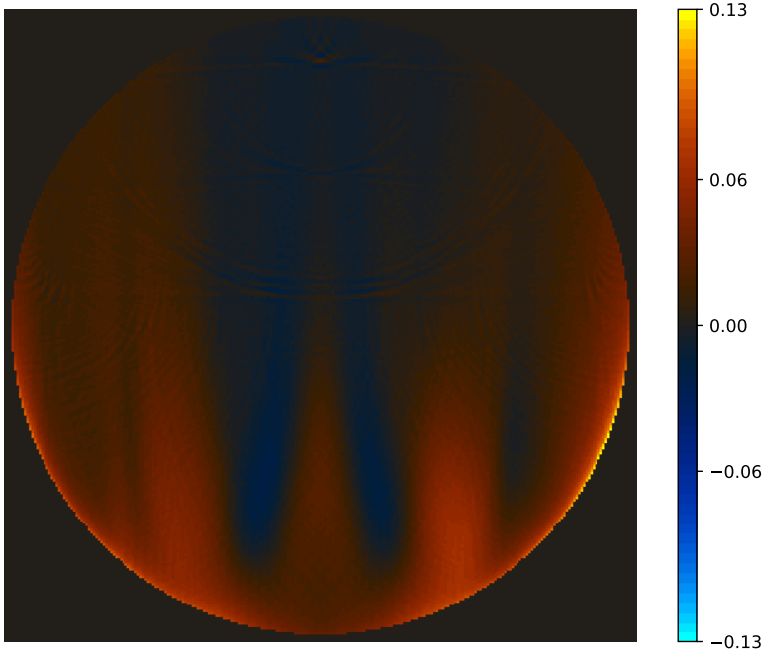

Difference between reduced reconstruction and full reconstruction

In practice, we have observed that the smooth difference is relatively small, but microlocal analysis yields no error estimates.
Moreover, small error is not guaranteed by these methods.

Thanks for listening!